Biochemical and Biophysical Research Communications **270,** 279–285 (2000)
doi:10.1006/bbrc.2000.2395, available online at http://www.idealibrary.com on IDEAL®

Engineering of a Mini-Trichosanthin That Has Lower Antigenicity by Deleting Its C-Terminal Amino Acid Residues

Siu-Hong Chan,*[,1] Pang-Chui Shaw,* Sandrine F. C. Mulot,* Li-Hui Xu,* Wah-Lun Chan,† Siu-Cheung Tam,† and Kam-Bo Wong*

**Department of Biochemistry and †Department of Physiology, Chinese University of Hong Kong, Shatin, N.T., Hong Kong, China*

Received February 15, 2000

Trichosanthin is a ribosome-inactivating protein that possesses antitumor and antiviral activities. Clinical trials of trichosanthin on AIDS patients, however, elicit anaphylactic reactions. To reduce the antigenicity of trichosanthin as a drug while preserving its biological activity, the C-terminal domain (residues 203 to 247), which contains a putative antigenic site, was systemically deleted. We have found that the minimum length of trichosanthin that can fold into an active conformation is residue 1 to 240. The mini-trichosanthin (C7) generated by deleting the last seven C-terminal amino acid residues has 2.7-fold decrease in antigenicity, 10-fold reduction in *in vitro* ribosome-inactivation activity, and *in vivo* cytotoxicity toward K562 cells, and 2-fold reduction in abortificient activity. Structural analyses of C7 indicate decrease in the helix content, increased exposure of Trp192, and lower thermodynamic stability. The deletion of the C-terminal residues (Leu241 to Ala247) probably perturbs local structure of the C-terminal antigenic epitope that results in the decrease in antigenicity and activities of C7.

Key Words: **antigenicity; ribosome-inactivating protein; protein structure; trichosanthin.**

Trichosanthin (TCS) is a type I ribosome-inactivating protein (RIP) isolated from the root tuber of *Trichosanthes kirilowii* Maximowicz. It is a single chain polypeptide possessing *N*-glycosidase activity that depurinates adenine 4324 of 28S rRNA. This renders the ribosome incapable of binding EF-2 and GTP so that protein synthesis is arrested (1). Our group has cloned the cDNA of trichosanthin (2), expressed it to high level (3) and investigated the role of some of the conserved residues in and around the active site (4, 5).

Clinically, trichosanthin has been used to induce mid-term abortion (6) and treat hydatiform mole (7). It has been linked to monoclonal antibody for attacking human hepatoma *in vitro* (8). Trichosanthin was the first RIP found to inhibit HIV-I *in vitro* (9–12), and clinical trials have been performed to evaluate its activity and safety for human administration. In a clinical trial on 22 patients with AIDS or AIDS-related complex, increase in $CD4^+$ and $CD8^+$ T cells was sustained for patients who received 36 and 50 μg/kg trichosanthin by constant intravenous infusion over 3 h (13). In another clinical trial, all patients showed increase $CD4^+$ T cell during a schedule of weekly and then monthly intravenous injection of 1.2 mg of trichosanthin in combination with other antiviral agents (14). Trichosanthin administration induced mild to severe anaphylactic responses in addition to neurological disorders. These include myalgia, nausea, diarrhea, and flu-like symptom (13, 14).

In view of this, we aim to engineer the protein to reduce its clinical side effects by reducing its antigenicity. Crystal structure of trichosanthin (15) indicates that the molecule has two domains: N-terminal domain (aa 1–202) and C-terminal domain (aa 203–247). There are three lines of evidence suggest that there is a prominent antigenic site at the C-terminal domain of trichosanthin: (i) computer modeling suggests an antigenic site composed of Ile201-Glu210 and Ile225-Asp229 of trichosanthin can be docked with an anti-TCS monoclonal IgE antibody (16); (ii) coupling of polyethylene glycol (PEG) to Gln219 significantly decrease the antigenicity of trichosanthin (17); (iii) peptide corresponds to aa 152–247 of trichosanthin is immuno-reactive to an anti-TCS polyclonal antibody (18). Since the C-terminal domain does not contain any active site residues, it is likely that deletion of this

[1] Present address: Division of Hematology, Department of Medicine, Johns Hopkins University School of Medicine, Baltimore, Maryland 21205.

0006-291X/00 $35.00

TABLE 1

Primers for PCR Mutagenesis of Trichosanthin

Protein	3′ primer sequence
rTCS	GGCGCGGATCCTATGCCATATTGTTTCTATTCAGCAG
C7	CACAGTGGATCCTACAGCAACGCGATGTTGGAGG
C8	CACAGTGGATCCTACAACGCGATGTTGGAGGTTAC
C9	CACAGTGGATCCTACGCGATGTTGGAGGTTAC
C21	GGCGCGGATCCTAGGTTATCGTGACTCGTTG
C35	GGCGCGGATCCTAAGGACTTTCAAACTGTCC
C45	ACAGTGGATCCTACGCTATCTGAATTTGCTTGG

Note. Sequence of 5′ primer is TGTGGCCATGGATGTTAGCTTC-CGTTTATCAGGTG. Sequences underlined represent *Nco*I and *Bam*HI sites of the 5′ primer and the 3′ primers, respectively.

domain may generate a less antigenic variant of trichosanthin while retaining its biological activities. In this study, we report the engineering of a mini-trichosanthin that has less antigenicity by deleting the C-terminal domain systematically.

MATERIALS AND METHODS

Materials. Restriction endonucleases and T4 DNA ligase were from New England Biolabs Inc. *Pfu* DNA polymerase was from Strategene. Rabbit reticulocyte lysate and L-[3,4,5-^{3}H(N)]-leucine were from Promega and NEN Life Science Products, respectively. Other chemicals were of analytical grade.

Construction of expression vectors and protein purification. PCR mutagenesis of trichosanthin using high fidelity *Pfu* DNA polymerase was carried out on pET58210 with the wild-type trichosanthin sequence (2). 3′ primers were designed to introduce appropriate deletions (Table 1). The PCR products were cleaved by *Nco*I and *Bam*HI and cloned to pET8c (3) for over-expression. The PCR-amplified DNA was sequenced by the T7 sequencing kit (Amersham Pharmacia Biotech.) to ensure no secondary mutation. Protein expression and purification were performed as described (4).

Antigenicity assay. The antigenicity of trichosanthin and C7 was assayed by competitive ELISA (19). Briefly, 100 μl of 5 μg/ml of mouse monoclonal anti-nTCS antibody IgE (TE1; kindly provided by Professor M. Yeh of Shanghai Institute of Cell Biology) was coated on the 96-well plate at 4°C overnight. The plate was then blocked with 1% BSA in PBS. 50 μl of samples was added and incubated at 37°C for 1 h. 50 μl of HRP-TCS (1:1000 diluted with 0.5% BSA in PBS-0.05% Tween 20) was added to each well and incubated at 37°C for 2 h. The plate was then washed with PBS-0.05% Tween 20 and 100 μl of substrate solution (0.8 mg/ml OPD in 0.2 M citrate-phosphate buffer, pH 5.0 containing 0.04% H_2O_2) was added to each well. After incubation at 37°C for 30 min, the reaction was terminated by 50 μl of 2.5 M H_2SO_4. The absorbance at 490 nm was read with a plate reader (Dynatech MR5000). All assays were done in duplicate. Antigenicity was represented by the concentration of the sample required to exhibit 50% inhibition (IC_{50}) of HRP-TCS binding to the IgE.

In vitro protein-synthesis inhibition activity assay. The ribosome-inactivating activities of the wild-type and variant trichosanthin were measured in an *in vitro* translation system using rabbit reticulocyte lysate (Promega Corporation, catalogue no. L4151) as described (20) with L-[3,4,5-^{3}H(N)]-leucine (NEN Life Science Products, catalogue no. NET460A) as label. Proteins of 3.7 pM to 37 nM and [^{3}H]-leucine of 5 nCi were incubated with the translation system at 30°C for 30 min in triplicate. Plots of [^{3}H]-leucine incorporation versus protein concentration were made for each protein and IC_{50} determined by fitting the curves to third-order regression.

Cytotoxicity assay. K562 cells (human erythroleukemia) were maintained in RPMI 1640 (GibcoBRL; containing 100 U/ml penicillin G sodium, 100 μg/ml streptomycin sulfate and 0.25 μg/ml amphoterin B) supplemented with 10% fetal calf serum. Cells were subcultured before they reached confluence so that actively growing cells were used for the assays. 0.1 ml of different concentration of trichosanthin and mutant was diluted in complete medium and added to 96-well plate. Equal volume (0.1 ml) complete medium containing 5×10^3 cells was added to each well except in the negative control. The cells were incubated at 37°C in a humidified atmosphere containing 5% CO_2 for 48 h. The cells were then pulsed for 6 h with [^{3}H]-thymidine (0.5 μCi/well). The cells were harvested and lysed onto glass fiber discs using a PHD cell harvester. The radioactivity that retained on the filters after washing with water and ethanol was measured in 2 ml of scintillation fluid using Beckman LS 7000 liquid scintillation counter. All assays were done in triplicate. Values of IC_{50} were estimated as the concentration of trichosanhin that causes 50% inhibition of [^{3}H]-thymidine incorporation.

Abortificient activity assay. Mature female mice were made pregnant by caging with fertile male mice. The presence of copulation plug in the following morning was designated as day 1 of pregnancy. At day 12 of pregnancy, C7 or wild-type trichosanthin were injected in the designated dosages. The mice were autopsied at day 14 of pregnancy. The total number of uterine implantation sites was recorded. The number of live fetuses, dead fetuses whose hearts had stopped pulsating, and resorbing fetuses were recorded. Mice were considered aborted when the number of dead fetuses exceed 50% of the total implantation sites.

Circular dichroism. CD spectra in the peptide region (200–250 nm) were measured by a Jasco J-715 spectropolarometer using a cylindrical sample cell of 1 cm path length at 20°C. The spectropolarometer was calibrated with d-10-camphorsulfonic acid at 290.5 nm. Concentrations of protein samples were determined by a modified Lowry method with bovine serum albumin as standards. The samples were adjusted to 2 μM in 10 mM Tris-Cl, pH 7.5 for data acquisition. Each protein was scanned three times from 200 to 250 nm and the spectra were averaged, subtracted from buffer blank spectrum and expressed as molar ellipticity, assuming mean residue weight of 110 per amino acid residue with adjustment of number of amino acid residues of each variant proteins. Deconvolution of CD spectra to alpha helix, beta sheet, turn and other conformations was done by the self-consistent method (21).

Equilibrium denaturation and fluorescence spectrometry. Fluorescence spectrometry was performed on an LS50B fluorescence spectrometer (Perkin–Elmer) and the data were analyzed using a fluorescence data manager software. Reversibility of unfolding of trichosanthin was determined by equilibrating 5 μM wild-type trichosanthin in 50 mM Tris-Cl, pH 7.2 with 7.6 M GnHCl for 2 h at 25°C and rapidly diluted to 0.5 μM in 50 mM Tris-Cl, pH 7.2. Control was done by diluting 5 μM wild-type trichosanthin in 50 mM Tris-Cl, pH 7.2 to 0.5 μM in 50 mM Tris-Cl, pH 7.2 for the same duration. Fluorescence spectra between 295 to 400 nm were scanned every 15 min.

To determine the equilibrium denaturation curves for trichosanthin, protein samples (0.5 μM) were treated with guanidine hydrochloride (GnHCl) at concentrations between 0 to 7.6 M in 50 mM Tris-Cl, pH 7.2. Each point was determined in a separate 1 or 2 mL solution. The protein samples were equilibrated with GnHCl solution at 25°C for 2 h prior to fluorescence measurement. The excitation wavelength was 280 nm and fluorescence spectra of each protein with or without 7.6 M GnHCl were also determined between 295 to 400 nm. Constant temperature in the cell (25°C) was ensured by circulating water from a water bath through the cell.

The equilibrium denaturation curves were analyzed by assuming a two-state folding mechanism. Fraction of protein unfolded (F_U) was

calculated from the observed fluorescence (Y) by: $F_U = (Y_F - Y)/(Y_F - Y_U)$, where Y_F and Y_U are the fluorescence intensities of the native and denatured states, respectively (22).

Free energy of unfolding ΔG_{H_2O} and the mid-point of unfolding $[GnHCl]_{1/2}$ were determined by plotting ΔG vs [GnHCl]:

$$\Delta G = \Delta G_{H_2O} - m[\text{GnHCl}],$$

where

$$\Delta G = -RT \ln \frac{F_U}{1 - F_U},$$

R is the ideal gas constant and T is the absolute temperature.

$[GnHCl]_{1/2}$ and ΔG_{H_2O} (the x and y intercepts, respectively) are determined by extrapolating the graph by linear regression. As the value of ΔG can only be measured accurately near the mid-point of transition, only ΔG values within ±1.5 kcal/mol were included in calculating $[GnHCl]_{1/2}$ and ΔG_{H_2O}.

RESULTS

Engineering of a Mini-Trichosanthin

Based on the secondary structure assignment by Zhou *et al.* (15), secondary structures of the C-terminal domain of trichosanthin was progressively deleted (Fig. 1). In variant C7, the C-terminal tail (aa 241–247, the last 7 residues), which is disordered and flexible as shown by X-ray crystallographic studies, was removed. In variant C21, helix H8 was further deleted (aa 227–247). In variant C35, strand S9 and S10 were deleted (aa 213–247). In variant C45, part of helix H7 and the loop region between H7 and S9 were further deleted (aa 203–247).

Of the 4 variants (C7, C21, C35 and C45) engineered, only C7 expressed as a soluble protein in *E. coli.* Variants C21, C35 and C45 expressed solely as insoluble inclusion bodies as judged by Western blotting and detection by anti-trichosanthin serum (data not shown). These three variants failed to refold from urea- or GnHCl-denatured inclusion bodies. Because variant C7 folded to a soluble conformation, further deletion was performed to delete the last 8 (aa 240–247) and 9 amino acid residues (aa 239–247) to see if deletion can be made further upstream of the sequence. Nevertheless, these two variants expressed solely as inclusion bodies (results not shown), showing that variant C7 is the mini-trichosanthin that can be folded to a soluble conformation. The aberrant folding of variants C21, C35, C45 and C8 suggest that aa 203–240 are required for the folding of trichosanthin. Variant C7 was purified to more than 95% purity and the yield was about 7 mg/L culture.

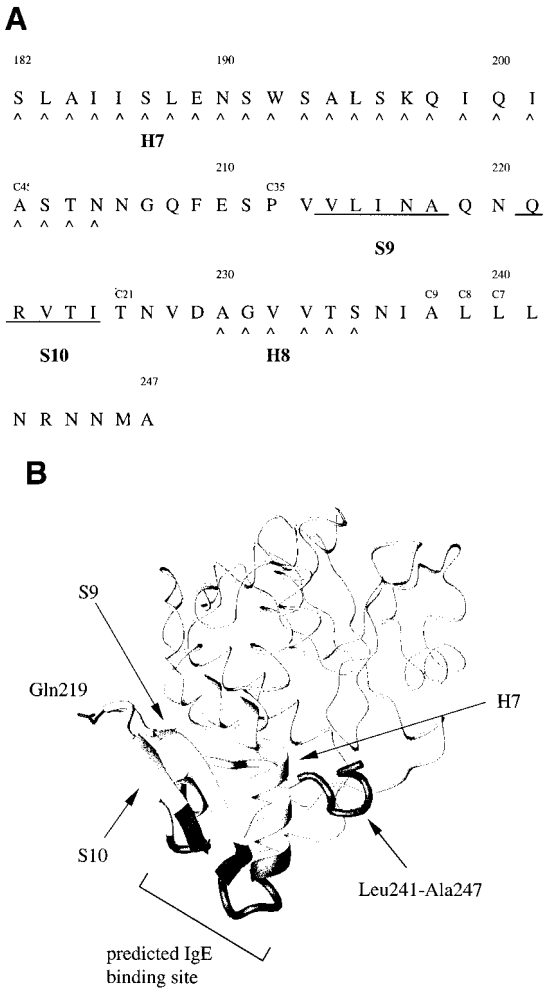

FIG. 1. Structure of the C-terminal domain of trichosanthin. (A) Sequence of trichosanthin starting from Ser182 was shown. Residues that constitute a helix (H7 and H8) are marked with a ^ at the bottom and those constitute a beta sheet strand (S9 and S10) are underlined. Assignment and numbering of alpha helix and beta sheet strands follows those made by Zhou *et al.* (1994). Residues with C45, C35, C21, C9, C8, and C7 printed on the top were the last residue of respective variants. (B) N-terminal domain (residue 1 to 181) are shown as thin ribbon and the C-terminal domain (residues 182 to 247) are shown in secondary structure render. Residues deleted in C7 (Leu241 to Ala247), Gln219 and the predicted monoclonal IgE binding site (15) are highlighted. It is noted that Leu241 is close to helix H7. Deletion of Leu241 to Ala247 may perturb the helical structure of H7 and reduces the helix content and the local structure of the C-terminal domain of C7.

Antigenicity of C7

The antigenicity of C7 and wild-type trichosanthin was assayed by their interaction with a monoclonal antibody IgE (TE1). By competitive ELISA, the antigenicity of C7 was found to decrease by 2.7-fold from the wild-type trichosanthin (Table 2). The results show that the antigenicity of trichosanthin can be reduced by deletion of the flexible C-terminal tail.

Biological Activity of C7

The *in vitro* ribosome-inactivating activity, *in vivo* cytotoxicity and abortificient activity of C7 and the wild-type trichosanthin were compared. As shown in

TABLE 2

Antigenicity of C7 and Wild-Type Trichsosanthin

	IC_{50} (μM)	Fold from rTCS
rTCS	0.12	1
C7	0.32	2.7

Note. The antigenicity of the wild-type trichosanthin and C7 are represented by concentration to exhibit 50% inhibition (IC_{50}) of HRP-TCS binding to monoclonal anti-TCS IgE antibody (TE1), which was predicted to dock at domain composes of Ile201-Glu210 and Ile225-Asp229 (He *et al.*, 1996).

Table 3, the *in vitro* ribosome-inactivating activity of C7 (IC_{50} = 0.18 nM) decreased from the wild-type (IC_{50} = 0.02 nM) by 9-fold. Its cytoxicity on K562 cells (IC_{50} = 2.01 nM) experiences a 12-fold decreased from the wild-type (IC_{50} = 0.16 nM). Although deletion of the last seven residues decreases its both *in vitro* and *in vivo* potencies by about 10-fold, C7 is still a potent ribosome-inactivating protein and cytotoxin that is effective in nanomolar range.

We have also assessed the abortificient activity of C7 in mice. The concentration of C7 required to attain 100% of aborted mice was 0.10 mg/25 g, compared to that of 0.05 mg/25 mg for the wild-type trichosanthin (Table 4). Thus, deleting the last 7 C-terminal residues of trichosanthin decreases the abortificient activity by 2-fold.

Structural Characterization

Secondary structures of C7 and wild-type trichosanthin were compared by circular dichroism (CD) spectroscopy (Fig. 2). The calculated values of alpha helix (0.22) and beta sheet content (0.48) of the wild-type trichosanthin agree well with those reported previously (23, 24) (0.29 and 0.43 for alpha helix and beta sheet, respectively) considering the differences in CD deconvolution methods and reference protein set used. Deletion of the last 7 amino acid residues of trichosanthin decreases the alpha helix content (0.14) and increases beta sheet content (0.56).

The fluorescence spectrum of the C7 and the wild-type trichosanthin were compared. The quantum yield of C7 is much lower than that of the wild-type and the emission maximum of C7 is red-shifted from 333 nm to 338 nm (Fig. 3). These findings suggest that Trp 192 (the only Trp in trichosanthin) is much solvent exposed in C7.

Relative stability of C7 and the wild-type trichosanthin were compared by equilibrium denaturation in guanidine hydrochloride (GnHCl). The unfolding process was followed by the fluorescence intensity in in-

TABLE 3

In Vitro Ribosome-Inactivating Activity and *in Vivo* Cytotoxicity of C7 and Wild-Type Trichosanthin

	IC_{50} of *in vitro* ribosome-inactivating activity (nM)	IC_{50} of K562 cytotoxicity (nM)
rTCS	0.02	0.16
C7	0.18	2.01

TABLE 4

Abortificient Activity of C7 and Wild-Type Trichosanthin

Dose (mg/25 g)	No. of mice	No. of dead fetuses/No. of implantation sites	% of aborted mice	No. of dead mice
TCS				
0.01	6	19/83 (22.9%)	16.7%	0
0.025	7	56/87 (64.4%)	85.7%	0
0.05	6	72/72 (100%)	100%	0
0.10	7	78/78 (100%)	100%	0
C7				
0.01	5	4/67 (5.9%)	0%	0
0.025	6	33/84 (26.2%)	0%	0
0.05	6	48/79 (60.8%)	66.7%	0
0.10	6	49/79 (62.0%)	100%	0

Note. Mice are considered aborted when the number of dead fetuses exceeded 50% of the total implantation sites on day 14 of pregnancy.

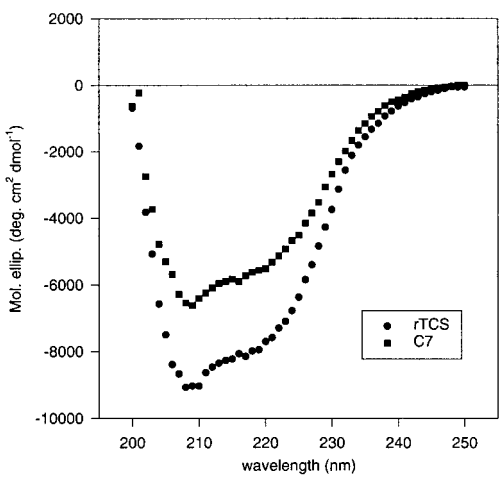

Protein	Alpha	Beta	Turn	Other	Sum
rTCS	0.24	0.45	0.12	0.19	0.9997
C7	0.14	0.56	0.10	0.19	0.9935

FIG. 2. CD spectra of C7 and wild-type trichosanthin. CD data were acquired between 200 to 250 nm that accounts for the peptide bond orientation. The far-ultraviolet CD was not made to 190 nm because of the lack of nitrogen-purging device for the sample cell. Each spectrum is plotted based on the average values of three consecutive scans with subtraction from the buffer blank. Data points in the short wavelength range having noise level higher than 500 V were eliminated.

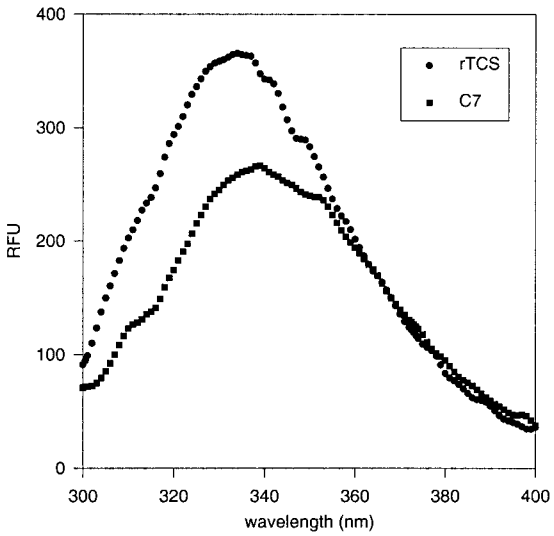

FIG. 3. Fluorescence spectra of C7 and wild-type trichosanthin. Five micromolar of wild-type or C7 trichosanthin was equilibrated at 25°C as described and excited at 280 nm. Emission spectra were acquired between 290 to 400 nm with slit sizes for both excitation and emission being 5 nm. The reduction of emission maximum and red-shift of C7 is probably due to exposure of Trp192 which is located on helix H7.

creasing concentration of GnHCl. We first established that the refolding of wild-type TCS and C7 is reversible. It has been reported that trichosanthin treated with 6 M GnHCl cannot be refolded by dialysis to a structure that possesses fluorescence properties, CD ellipticity and endonuclease activity comparable to the control (25). In our hand, we noticed that prolonged dialysis adversely affected the fluorescence emission value and *in vitro* ribosome-inactivating activity of trichosanthin. However, we have shown here that trichosanthin can be refolded by rapid dilution. TCS was denatured in 7.6 M GnHCl and then refolded by diluting the denatured protein solution ten times (see Materials and Methods). The fluorescence spectra of the refolded trichosanthin are similar to that of the control (native trichosanthin without the treatment of GnHCl) (Fig. 4), suggesting refolding of both wild-type trichosanthin and variant C7 is reversible.

From the equilibrium denaturation experiment, wild-type trichosanthin is a quite stable protein (ΔG_{H_2O} = 6.8 kcal/mol; $[GnHCl]_{1/2}$ = 5.3 M). Deletion of the last 7 residues reduces the ΔG_{H_2O} and $[GnHCl]_{1/2}$ to 1.8 kcal/mol and 1.5 M, respectively (Fig. 5).

DISCUSSION

As a therapeutic protein, administration of trichosanthin to patients elicits anaphylactic reactions. To reduce the antigenicity of trichosanthin, we systematically deleted the C-terminal domain which carries a prominent antigenic epitope. Deletions were designed so that the major secondary structures and the flexible C-terminal tail were progressively removed. Our results indicate that the whole C-terminal domain cannot be deleted because the secondary structures of the domain are required for folding of trichosanthin. Nevertheless, the flexible tail comprising of the last 7 amino acid residues at the C-terminus (aa 241–247) can be deleted and the variant (C7) retains the biological activities of trichosanthin and exhibits decreased antigenicity. C7 (aa 1–240) appears to be the minimum length of trichosanthin that can be folded. Further deletion of Leu240 in variant C8 disrupted the folded structure.

We succeeded in generating a mini-trichosanthin that has lower antigenicity by deleting the last 7 amino acid residues of the C-terminus. The antigenicity of this variant C7 decreases by 2.7-fold from the wild-type. Although the *in vitro* ribosome-inactivating activity and *in vivo* cytotoxicity of C7 decrease by 10-fold from the wild-type, it is still a potent ribosome-inactivating protein (IC_{50} = 0.18 nM) and cytotoxin (IC_{50} = 2.01 nM) that is effective in nM range. Its *in vitro* ribosome-inactivating activity are comparable to that of ricin A-chain and pokeweed antiviral protein, which have IC_{50} values of 0.1 and 0.2 nM, respectively (26).

Structural analyses suggest that deletion of the C-terminal tail results in: (i) decrease in helix content, (ii) increase solvent-exposure of Trp192, (iii) reduced thermodynamic stability. Deletion of the last 7 residues apparently causes structural changes that account for the observed decreases in antigenicity and biological activities. Trp 192 is located on helix H7,

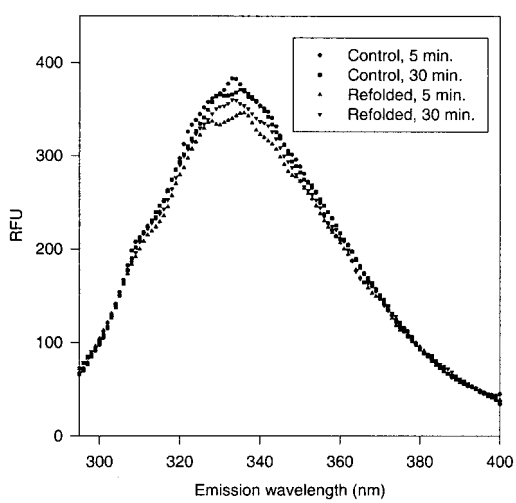

FIG. 4. Reversibility of GnHCl denaturation of trichosanthin. Wild-type trichosanthin was equilibrated in 7.6 M GnHCl and then rapidly diluted in Tris–HCl buffer to refold the protein as described. Trichosanthin equilibrated in Tris–HCl buffer was diluted in the same way as a control. Emission spectra of the control and refolded trichosanthin at 5 and 30 min after dilution are shown. The spectra of refolded and control trichosanthin are essentially identical.

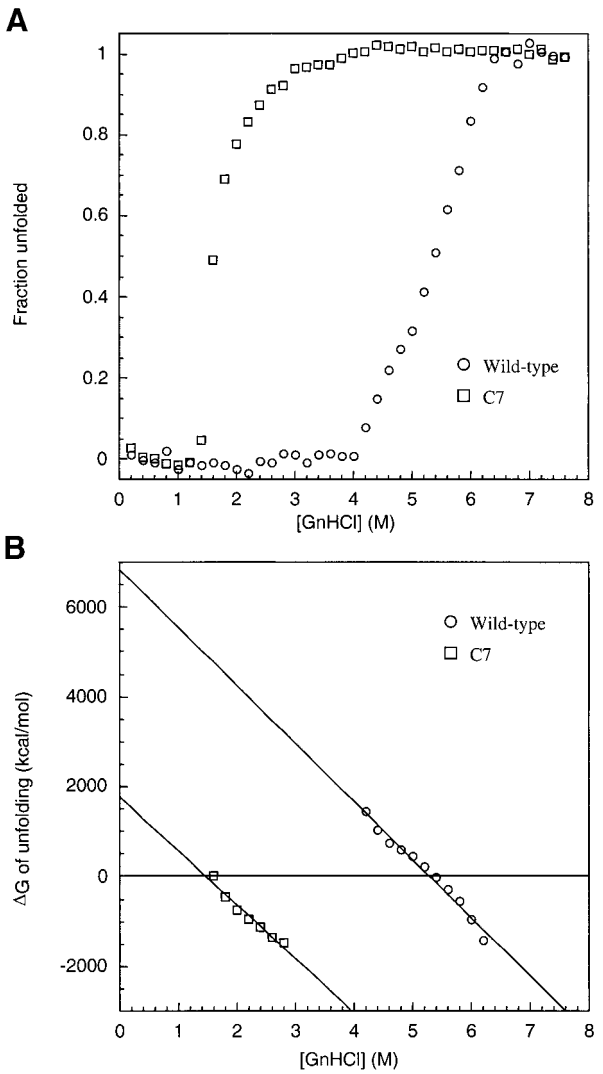

FIG. 5. Unfolding of C7 and wild-type trichosanthin. Proteins were equilibrated with different concentration of GnHCl at 25°C for two h before measurement. Plots of fraction unfolded (A) and free energy (ΔG) of unfolding as a function of GnHCl concentration are shown. The mid-point of unfolding for wild-type trichosanthin and C7 are 5.3 and 1.5 M GnHCl, respectively, and the ΔG_{H_2O} values are 6.8 and 1.8 kcal/mol for wild-type trichosanthin and C7, respectively.

which is in contact with the C-terminal tail. Taken together, removal of the C-terminal tail may perturb the helical structure of H7 and result in a decrease in helix content of C7 and a more solvent exposed Trp 192. The exact binding site of the monoclonal IgE is not known. The decrease in antigenicity of C7 can be due to the fact that the IgE interacts directly with the C-terminal tail. It is also possible that the deletion perturbs the local structure of the C-terminal domain in a way that the IgE binds less efficiently to C7. The lower stability of C7 suggests that the altered structure may be a slightly unfolded state of trichosanthin. X-ray crystallographic analysis of C7 is in progress to obtain more structural information of this variant.

Our approach of deleting the C-terminal residues reduces the antigenicity of trichosanthin by altering the local structure of the C-terminal antigenic epitope. It may be applicable to other RIPs because their tertiary structures are highly homologous. On the other hand, because antibodies of homologous RIPs do not cross-react with other, the antigenic determinant of RIP may reside in individual amino acid residues not conserved among RIPs. We may further reduce the antigenicity of trichosanthin by deleting or mutating the nonconserved but exposed residues of the variant C7. Recent report of residues not required for activity in ricin A-chain (27) provides a reference for the selection. Also, the small domain constituted by beta strands S9 (aa 214–218), S10 (aa 221–225) and a two-residue loop containing Gln219 (Fig. 1B), which are close to the predicted docking site of the monoclonal antibody TE1 (aa 201–210; aa 225–229), may be modified. Given the similarity in tertiary structure of RIPs, the importance of aa 203–240 in the folding of trichosanthin suggests that trichosanthin, and other RIP, appear to be highly evolved in such a way that only few residues at the C-terminal region can be deleted without affecting the structure or function.

ACKNOWLEDGMENTS

Thanks are due to Dr. X. H. He for his assistance in the cytotoxicity and antigenicity assay. We also thank the Department of Chemistry of the Chinese University for allowing us to use their CD spectropolarometer J-715. This work was supported by a grant (CUHK 4039/98M) from the Research Grants Council of Hong Kong.

REFERENCES

1. Endo, Y., Gluck A., Chan, Y. L., Tsurugi, K., and Warl, I. G. (1990) RNA–protein interaction. *J. Biol. Chem.* **265,** 2216–2222.
2. Shaw, P. C., Yung, M. H., Zhu, R. H., Ho, W. K. K., Ng, T. B., and Yeung, H. W. (1991) Cloning of trichosanthin cDNA and its expression in *Escherichia coli. Gene* **97,** 267–272.
3. Zhu, R. H., Ng, T. B., Yeung, H. W., and Shaw, P. C. (1992) High level synthesis of biologically active recombinant trichosanthin in *E. coli. Int. J. Peptide Protein Res.* **39,** 77–81.
4. Wong, K. B., Ke, Y. B., Dong, Y. C., Li, X. B., Guo, Y. W., Yeung, H. W., and Shaw, P. C. (1994) Structure/function relationship study of Gln156, Glu160 and Glu189 in the active site of trichosanthin. *Eur. J. Biochem.* **221,** 787–791.
5. Shaw, P. C., Mulot, S., Ma, S. K., Xu, Q. F., Yao, H. B., Wu, S., Lu, X. H., and Dong, Y. C. (1997) Structure/function relationship study of Tyr14 and Arg22 in trichosanthin, a ribosome-inactivating protein. *Eur. J. Biochem.* **245,** 423–427.
6. Liu, G., Liu, F., Li, Y., and Yu, S. (1985) A summary of 402 cases of termination of early pregnancy with crystalline preparation of trichosanthi. *In* Advances in Chinese Medicinal Materials Research (Cheung, H. M., Yeung, H. W., Tso, W. W., and Koo, A., Eds.), pp. 327–333, World Scientific Publishing Co., Singapore.
7. Lu, P. X., and Jin, Y. C. (1990) Trichosanthin in the treatment of hydatiform mole. Clinical analysis of 5 cases. *Chinese Med. J.* **103,** 183–185. [in English]
8. Wang, Q. C., Ying, W. B., Xie, H., Zhang, Z. C., Yang, Z. H., and Ling, L. Q. (1991) Trichosanthin-monoclonal antibody conjugate

specifically cytotoxic to human hepatoma cells *in vitro*. *Cancer Res.* **51,** 3353–3355.

9. McGrath, M. S., Hwang, K. M., Caldwell, S. E., Gaston, I., Luk, K. C., Wu, P., Ng, V. L., Crowe, S., Daniels, J., Marsh, J., Deinhart, T., Lekas, P. V., Vennari, J. C., Yeung, H. W., and Lifson, J. D. (1989) GLQ223: An inhibitor of human immunodeficiency virus replication in acutely and chronically infected cells of lymphocytes and mononuclear phagocyte lineage. *Proc. Natl. Acad. Sci. USA* **86,** 2844–2848.
10. McGrath, M. S., Santulli, S., and Gaston, I. (1990) Effects of GLQ223 on HIV replication in human monocyte/macrophages chronically infected *in vitro* with HIV. *AIDS Res. Hum. Retroviruses* **6,** 1039–1043.
11. Pan, L. Z., and Levy, J. A. (1994) Inhibition of HIV replication by trichosanthin in peripheral blood mononuclear cells. *Curr. Ther. Res.* **55,** 718–727.
12. Shaw, P. C., Chan, W. L., Yeung, H. W., and Ng, T. B. (1994) Minireview: Trichosanthin—A protein with multiple pharmacological properties. *Life Sci.* **55,** 253–262.
13. Kahn, J. O., Gorelick, K. J., Gatti, G., Arri, C. J., Lifson, J. D., Gambertoglio, J. G., Bostrom, A., and Williams, R. (1994) Safety, activity, and pharmacokinetics of GLQ223 in patients with AIDS and AIDS-related complex. *Antimicrob. Agent Chemother.* **38,** 260–267.
14. Byers, Y. S., Levin, A. S., Malvino, A., Waites, L., Robins, R. A., and Baldwin, R. W. (1994) A phase I/II study of trichosanthin treatment of HIV disease. *AIDS Res. Hum. Retroviruses* **10,** 413–420.
15. Zhou, K., Fu, Z., Chen, M., Lin, Y., and Pan, K. (1994) Crystal structure of trichosanthin at 1.88Å resolution. *Protein Struct. Funct. Genet.* **19,** 4–13.
16. He, Y. N., Xia, Z. X., Wang, Y., Ji, Y. Y., and Yeh, M. (1996) Prediction of antigenic determinants of trichosanthin by molecular modelling. *Cell Res.* **6,** 93–100
17. He, X. H., Shaw, P. C., and Tam, S. C. (1999) Reducing the immunogenicity and improving the *in vivo* activity of trichosanthin by site-directed PEGylation. *Life Sci.* **65,** 355–368.
18. Mulot, S., Chung, K. K., Li, X. B., Wong, C. C., Ng, T. B., and Shaw, P. C. (1997) The antigenic sites of trichosanthin, a ribosome-inactivating protein with multiple pharmacological properties. *Life Sci.* **61,** 2291–2303.
19. Nie, H., Cai, X, He, X. i, Xu, L., Ke, X., Ke, Y., and Tam S.-C. (1998) Position 120–123, a potential active site of trichosanthin. *Life Sci.* **62,** 491–500
20. Yeung, H. W., Li, W. W., Feng, A., Baribieri, L., and Stirpe F. (1988) Trichosanthin, alpha-momorcharin and beta-mormorcharin: Identity of abortificient and ribosome-inactivating proteins. *Int. J. Peptide Protein Res.* **31,** 265–268.
21. Sreerama, N., and Woody, R. W. (1993) A self-consistent method for the analysis of protein secondary structure from circular dichroism. *Anal Biochem.* **209,** 32–44.
22. Pace, C. N., and Scholtz, J. M. (1996) Measuring the conformational stability of a protein. *In* Protein Structure: A Practical Approach (Creighton, T. E., Ed.), pp. 299–320, IRL Press, NY.
23. Kubota, S., Yeung, H. W., and Yang, J. T. (1986) Conformation of abortifacient proteins: Trichosanthin, α-momorcharin and β-momorcharin. *Biochim. Biophys. Acta* **871,** 101–106.
24. Kubota, S., Yeung, H. W., and Yang, J. T. (1987) Conformation similarities of ricin A-chain and trichosanthin. *Int. J. Peptide Protein Res.* **30,** 646–651.
25. Lau, C. K., Wong, R. N. S., Lo, S. C. L., and Kwok, F. (1998) Refolding of denatured trichosanthin in the presence of GroEL. *Biochem. Biophys. Res. Commun.* **245,** 148–154.
26. Barbieri, L., Battelli, M. G., and Stripe, F. (1993) Ribosome-inactivating proteins from plants. *Biochim. Biophys. Acta* **1154,** 237–282.
27. Kitaoka, Y. (1998) Involvement of the amino acids outside the active-site cleft in the catalysis of ricin A chain. *Eur. J. Biochem.* **257,** 255–262.